MINISTRY OF SUPPLY

AERONAUTICAL RESEARCH COUNCIL
REPORTS AND MEMORANDA

A Theoretical Approach to the Design of Hydrofoils

By

C. H. E. WARREN, M.A.

LONDON: HER MAJESTY'S STATIONERY OFFICE

1953

PRICE 5*s* 6*d* NET

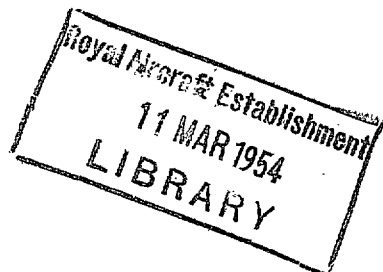# A Theoretical Approach to the Design of Hydrofoils

By

C. H. E. WARREN, M.A.

Reports and Memoranda No. 2836*

September, 1946

Summary.—An investigation has been made into the application of the theory of thin sections to the design of hydrofoils having high cavitation speeds. Consideration is given to both symmetrical sections, which themselves are suitable for struts, and camber-lines, which, when used with the symmetrical sections, lead to cambered sections which are suitable for lifting surfaces. In all the aim has been to keep the peak local velocities to a minimum, and the sections developed differ from ' low-drag ' aerofoil sections mainly in that, being hydrofoils, the sections have sharp leading edges.

The theoretical optimum section consists of an elliptic symmetrical section superimposed on a logarithmic camber-line. Typical practical sections will cavitate at a speed lower by about 5 knots than the theoretical optimum section of the same thickness/chord ratio and at the same lift coefficient. For strut sections it is shown that sections having high cavitation speeds at zero incidence tend to be inferior to other sections at incidences as small as 2 deg. For lifting surface sections it is shown that although a high cavitation speed demands a low design lift coefficient, a high loading at cavitation demands a high design lift coefficient.

Operation above cavitation speeds or over wide ranges of lift coefficient are not considered.

---

1. *Introduction.*—The theoretical approach to the design of hydrofoil sections follows very closely that of aerofoils with good compressibility characteristics. There are, however, a few characteristics peculiar to the hydrofoil which make separate consideration necessary. In this investigation consideration is given to the design of symmetrical and cambered sections which have high cavitation speeds. Such sections are suitable for struts and lifting surfaces respectively. It will be assumed that the hydrofoils are sufficiently immersed for the undisturbed flow to be treated as a uniform stream of infinite extent.

2. *The Theory of Thin Sections.*—Before proceeding to the design of hydrofoil sections having high cavitation speeds, it will be useful to consider the theory upon which such design is based. A high cavitation speed can be obtained by designing that the peak suction (or peak local velocity, which is related to it by Bernoulli's equation) shall be as low as possible. It will be useful, therefore, to consider first of all the relation between section shape and velocity distribution.

Let the ordinates of the upper and lower surfaces of a typical section at station x be y_u and y respectively, where the chord-line is taken as the x-axis. (*See* Fig. 1.)

Let	$y_c = \frac{1}{2}(y_u + y_l),$
and	$y_t = \frac{1}{2}(y_u - y_l).$
Then	$y_u = y_c + y_t ,$
and	$y_l = y_c - y_t .$

A

The typical section can be considered, therefore, as a combination of a symmetrical section with ordinates $\pm\, y_t$ superimposed upon a camber-line (or asymmetrical section of zero thickness) with ordinates y_c. (*See* Fig. 1.)

The velocity distribution on a symmetrical section at zero incidence is the same on both the upper and lower surfaces. The velocity distribution on an isolated camber-line at any incidence is such that, to the first order, the velocity increment on the upper surface is equal to the velocity decrement on the lower surface[1].

The velocity distribution of a typical section is obtained, to the first order, by adding the velocity increments due to the symmetrical section at zero incidence and the velocity increments due to the camber at the particular incidence being considered. If the stream velocity is U_0 and the velocity increments due to the symmetrical section at zero incidence, and due to the camber at incidence α are u_t and $\pm\, u_c$ respectively, then the velocity increments, u_u and u_l, at points on the upper and lower surfaces of the typical section are given by

$$u_u = u_t + u_c$$
$$u_l = u_t - u_c .$$

Clearly
$$u_c = \tfrac{1}{2}(u_u - u_l)$$
and
$$u_t = \tfrac{1}{2}(u_u + u_l).$$

This approach to the problem, which is applicable only to thin sections of small camber, is explained more fully by Squire[1], and is illustrated diagrammatically in Fig. 1.

Because the velocity distribution, and hence the pressure, is the same on both surfaces, a symmetrical section at zero incidence produces no lift. Thus the lift of a typical section is due entirely to the pressure associated with the velocity distribution, u_c, due to the camber and incidence. This indicates how a typical section may be designed. Firstly, to obtain the hydrodynamic lift required, a suitable camber-line having ordinates y_c is designed, such that when it is set at the proper incidence, the required lift is obtained. This proper incidence is called the 'ideal angle of incidence', and the lift coefficient corresponding to this incidence is called the 'design lift coefficient'. When set at the ideal angle of incidence the camber-line will give rise to velocity increments $\pm\, u_c$. Secondly, to obtain the necessary structural strength a symmetrical section, or thickness distribution, having ordinates $\pm\, y_t$ is superimposed on the camber-line. This gives rise to the velocity increments u_t. We see, therefore, that the velocity distribution of a typical section is due partly to the camber and incidence which are necessary to produce lift, and partly to the thickness distribution, which is necessary to provide structural strength.

3. *The Theoretical Optimum Section for High Cavitation Speed.*—Bernoulli's equation for incompressible flow is

$$p + \tfrac{1}{2}\varrho U^2 - g\varrho z = p_0 + \tfrac{1}{2}\varrho U_0{}^2$$

where U_0 is the stream velocity,

U is the local velocity,

p_0 is the pressure at the free surface of the water,

p is the local pressure,

ϱ is the density,

g is the acceleration due to gravity,

z is the depth below the undisturbed free surface.

2

Cavitation occurs when the local pressure p falls to p_v, the vapour pressure of water at that temperature. The corresponding critical value of the local velocity U is given by

$$\left[\left(\frac{U}{U_0}\right)_{\text{crit}}\right]^2 = 1 + \frac{p_0 - p_v + g\varrho z}{\frac{1}{2}\varrho U_0{}^2}.$$

The ratio $(U/U_0)_{\text{crit}}$ is shown for a range of values of stream velocity U_0 and depth z in Fig. 2. This figure shows that to avoid cavitation at a forward speed of, say, 60 knots, the local velocity ratio must not exceed about $1 \cdot 1$. As the maximum velocity in a stream occurs on the boundary, the problem of designing a hydrofoil for a high cavitation speed reduces to that of designing for a small value of the peak velocity ratio on its surface.

The section having the highest possible cavitation speed is the flat plate at zero incidence. The velocity on the surfaces is equal to the stream velocity everywhere, and the cavitation speed is, therefore, infinite. The flat plate at zero incidence is unsuitable as a hydrofoil section, however, because it produces no lift, and has no structural strength. As was pointed out in section 2 lift can be produced by cambering and by incidence, and structural strength can be obtained by thickening.

To the first order, the velocity increment distributions on symmetrical sections of ' similar ' shape are proportional to the thickness, and likewise the velocity increment distributions on camber-lines of ' similar ' shape are proportional to the camber and hence to the lift. (This follows from the additive property of thin sections of small camber). As a first measure, therefore, a low peak velocity can be attained by designing for small thickness and low lift. Having decided on the maximum thickness and lift, it is possible that the peak velocity increment can be further reduced by refinements in section shape. These are the problems to be investigated here.

The problems may be put more definitely as follows. What symmetrical section has the lowest possible peak velocity increment for a given maximum thickness, and what camber-line at a suitable incidence has the lowest possible peak velocity increment for a given design lift coefficient ? The answers to these problems have already been found in connection with the design of aerofoils having good compressibility characteristics[1,2]. They are :—

Symmetrical section : The elliptic symmetrical section, having equation $y_t = t\sqrt{[x\,(1 - x)]}$, where t is the maximum thickness divided by the chord. This section has, to the first order, a constant velocity increment over both surfaces given by $u_t = tU_0$, except at the leading and trailing edges, which are singular points.

Camber-line : The logarithmic camber-line, having equation .

$$y_c = - [C_L/4\pi][x \log x + (1 - x) \log (1 - x)],$$

where C_L is the design lift coefficient. This line, has to the first order, a constant velocity increment on the upper surface given by $u_c = \frac{1}{4}C_L U_0$, and an equal velocity decrement on the lower surface, except at the leading and trailing edges, which are again singular points. The ideal angle of incidence is 0 deg.

In these two cases it will be noticed that the velocity increments are constant along the chord. Such distributions are spoken of as ' flat-topped ', and clearly there is no peak as such.

The equation of a section of maximum thickness/chord ratio t and design lift coefficient C_L, having theoretically the highest possible cavitation speed is, therefore,

$$y = - [C_L/4\pi][x \log x + (1 - x) \log (1 - x)] \pm t\sqrt{[x(1 - x)]} .$$

3

The velocity increment distribution for this section is given by

$$u = U_0(t \pm \tfrac{1}{4}C_L) .$$

Owing to the flat-top nature of the velocity distribution, the cavitation speed of this section is determined by the velocity increment, $u_u = U_0(t + \tfrac{1}{4}C_L)$, which occurs over the whole upper surface.

4. *Practical Sections having High Cavitation Speeds.*—4.1. *General Considerations.*—There are objections to the use of the theoretical optimum section, developed in section 3, as a hydrofoil section. In the first place a sharp trailing edge is desirable to avoid a breakaway from the rear[2]. A sharp leading edge, also, is desirable to give good characteristics when the foil breaks the surface, because a round leading edge throws up considerably more spray than a sharp leading edge. Moreover the logarithmic camber-line is unsuitable because it is desirable to reduce the chordwise loading near the trailing edge[1], and thus avoid an excessive pitching moment[2]. In sections 4.2, 4.3, below we shall derive symmetrical sections and camber-lines that are not subject to these objections.

4.2. *Symmetrical Sections.*—Using the methods of thin-aerofoil theory given by Squire[1] three sections have been derived for which the velocity is constant over most of the chord, but which falls off linearly at the leading and trailing edges, from points roughly 5, 10, 15 per cent of the chord from the edges, the amount of fall-off being adjusted to make the edges sharp. The mathematical analysis is given in Appendix I, and the sections derived are given in Table 1 and shown in Fig. 3.

These sections have cuspidal leading and trailing edges, and for all the value of $(U/U_0)_{max}$ is $1 \cdot 1$. The thickness/chord ratios are respectively $9 \cdot 62$, $9 \cdot 26$ and $8 \cdot 78$ per cent. It was considered that cuspidal edges were undesirable in practice, and accordingly the cusps were removed by making the sections straight over roughly the initial and final 5, 10, and 15 per cent of the chord respectively. In their modified form the sections have been designated the 25 deg section, 35 deg section and 45 deg section respectively, from the main parameter in their derivation given in Appendix I. Ordinates of these modified sections, scaled to a thickness/chord ratio of 10 per cent, together with those of the elliptic section and a section formed by two circular-arcs, are given in Table 2 and are shown in Figs. 4, 5, 6, 7, 8. The circular-arc section is presented as a section that is in fairly common usage as a hydrofoil section. Also shown in Figs. 4, 5, 6, 7, 8 are the exact velocity distributions calculated by the method of Theodorsen[3], for incidences of 0 deg, 2 deg, 5 deg.

4.3. *Camber-Lines.*—Squire[4] has given a number of camber-lines which have a velocity distribution in which the velocity is constant up to a certain point along the chord, and then falls linearly to the stream velocity at the trailing edge. These camber-lines are, however, unsuitable for use with symmetrical sections having a sharp leading edge because they would lead to sections having a concavity on the lower surface near the leading edge.

Using the method developed by Jacobs[5], and quoted by Squire[1], camber-lines have been developed which have a velocity distribution in which the velocity is constant between two definite points of the chord, and falls linearly to the stream velocity from these points to the leading and trailing edges. The fall-off to the leading edge has been made from the points $0 \cdot 05c$, $0 \cdot 1c$ and $0 \cdot 15c$. The fall-off to the trailing edge has been made from the points $0 \cdot 5c$, $0 \cdot 6c$, $0 \cdot 7c$, $0 \cdot 8c$, $0 \cdot 85c$, $0 \cdot 9c$, and $0 \cdot 95c$. For convenience the camber-line for which the fall-offs have been made from, say, the $0 \cdot 05c$ point and the $0 \cdot 6c$ point respectively, has been designated the $(0 \cdot 05 - 0 \cdot 6)$ camber-line. The mathematical analysis is given in Appendix II, and the camber-lines derived are given in Tables 3, 4, 5, scaled to a design lift coefficient of $1 \cdot 0$.

5. *Comparison of the Practical Sections with the Theoretical Optimum Section.*—5.1. *Strut Sections.*—We will consider the suitability as strut sections of the ellipse and the four practical symmetrical sections given in Table 2 and shown in Figs. 4, 5, 6, 7, 8. The ellipse, with its

4

uniform velocity distribution, represents the best that can be achieved, and provides a measure for assessing other sections. The cavitation speeds* at zero incidence, for the ellipse, the .35 deg section and the circular-arc are shown as a function of thickness/chord ratio in Fig. 9, which brings out the fact that greater gains in cavitation speed are to be had by reduction of thickness/ chord ratio than from attention to section shape.

At incidences other than zero all the sections other than the ellipse have, theoretically, infinite velocity (corresponding to infinite negative pressure) at the leading edge. Available evidence suggests that in practice very high peak pressures do not occur. Even should a high local peak pressure induce local cavitation, it is probable that such cavitation would be very localised[6] owing to the fact that, as shown in Figs. 5, 6, 7 and 8 in most cases there is a favourable (decreasing) pressure gradient a short distance behind the leading edge.

We suppose, therefore, that in the case of the sections with sharp leading edges, the main onset of cavitation at small incidences will occur when the local velocity at the second peak (which occurs at from 7 per cent to 40 per cent. of the chord, depending on the section) becomes critical. In the table below the critical values of U/U_0 and the corresponding cavitation speeds are given for the five sections for a thickness/chord ratio of 10 per cent at incidences of 0 deg and 2 deg. At an incidence of 5 deg the regions of high pressures at the leading edge are probably too extensive for their presence to be ignored in determining the onset of cavitation.

Incidence (deg)	Section				
	Ellipse	25 deg	35 deg	45 deg	Circular-arc
	$(U/U_0)_{crit}$				
0	1·100	1·106	1·111	1·118	1·132
2	1·34	1·23	1·20	1·18	1·175
	Cavitation speed (knots)				
0	59	57½	56	54½	51
2	30½	38	41	43	44

The interesting fact shown by this table is that the ellipse ceases to have good cavitation properties at incidences other than zero, whereas the sections with poorer characteristics at zero incidence, have better properties by comparison at incidences of 2 deg. In particular the circular-arc shows up particularly favourably.

5.2. *Lifting-surface Sections.*—For lifting-surface sections there are two criteria which might be used to assess the merits of hydrofoil sections with regard to their cavitation characteristics, each of which is of interest. The first criterion asks the question ' What is the highest speed that the hydrofoil can attain before cavitation occurs ? ' and the second asks ' What is the greatest load that the hydrofoil can support before cavitation occurs ? ' It is felt that the first criterion would be used in assessing the merits of hydrofoils for high-speed naval craft, but the second is of interest in connection with the take-off of seaplanes, where it may be desirable to lift the hull out of the water before cavitation starts.

The speeds and loadings at cavitation are shown in Figs. 10 and 11 respectively for a good practical series of hydrofoil sections and for the theoretical optimum series, each set at the appropriate ideal angle of incidence. The practical section chosen for this purpose was the 35 deg symmetrical section given in Table 2 superimposed on the (0·05–0·6) camber-line given in Table 3. A typical section of this series, together with corresponding theoretical optimum section, is shown in Fig. 12.

---

* The cavitation speeds quoted in the text will refer to zero depth, a pressure of 760 mm of mercury and a temperature of 15 deg C.

A*2

Fig. 10 shows that the practical sections will have a cavitation speed about 5 knots lower than that of the theoretical optimum section. Fig. 10 also brings out the fact that the cavitation speed can be increased by reducing both the thickness/chord ratio and the design lift coefficient, 65 knots being attainable with a good practical section of thickness/chord ratio 5 per cent designed for a lift coefficient of $0 \cdot 1$.

Fig. 11, on the other hand, shows that the loading at cavitation can be increased by reducing the thickness/chord ratio, and by increasing the design lift coefficient. Actually there is an optimum design lift coefficient which yields maximum loading for any thickness/chord ratio, but these optima occur at lift coefficients that are too high for the theory to be valid: the theoretical optimum lift coefficients are greater than $1 \cdot 0$ for thickness/chord ratios greater than 5 per cent. Fig. 11 shows that a foil loading of about 15 lb/sq in. should be attainable without cavitation on a hydrofoil of thickness/chord ratio 5 per cent provided that it is designed for a sufficiently high lift-coefficient, of about $0 \cdot 5$, say. The speed of cavitation will be low, and can, of course, be obtained from Fig. 10. For the case quoted it would be about 40 knots. The loading on a section designed for a high cavitation speed, say 65 knots (design lift coefficient $= 0 \cdot 1$), would be only 8 lb/sq in.

At incidences other than the ideal, or, in other words, at lift coefficients other than the design lift coefficient, the characteristics of a section depend upon the peak-velocity increment at this lift coefficient, which can be found by a method such as Theodorsen's[3]. All that will be said here is that this peak velocity increment would certainly be greater than the peak velocity increment of the section of the series specifically designed for that lift coefficient. For example, the cavitation speed of the practical section shown in Fig. 11 at a lift coefficient of say, $0 \cdot 1$, would, from Fig. 10, certainly be less than 45 knots and, likewise, from Fig. 11, the loading would be less than 4 lb/sq in.

6. *Further Considerations.*—In our assessment of the merits of various sections the speed at which the onset of cavitation occurs has been used as a criterion. In other words, the sections have been designed to avoid the onset of cavitation. It is possible that the characteristics above the cavitation speed could be improved by designing for this regime. Moreover, the relative merits have been based, in the main, on the characteristics at the ideal angle of incidence. If a specially wide range of incidences were required, other sections might give better performance. For example, it might be profitable to consider a ' roof-top ' velocity distribution, with the peak far back, rather than the flat-top distributions considered here.

It must be also borne in mind that, in the calculations made here, it has been assumed that the undisturbed flow is a uniform stream of infinite extent. In other words, effects due to the fact that hydrofoils may in fact be operating just below a free surface have been ignored.

7. *Conclusions.*—Sections have been derived which should have good characteristics as hydrofoil strut and lifting-surface sections, and they have been compared with the theoretical optimum symmetrical section, superimposed on a logarithmic camber-line. The practical sections will cavitate at a speed lower by about 5 knots than the theoretical optimum section of the same thickness/chord ratio and at the same lift coefficient.

For struts a suitable symmetrical section at zero incidence will delay the onset of cavitation to a speed of about 55 knots for a thickness/chord ratio of 10 per cent, and to about 80 knots for a thickness/chord ratio of 5 per cent. At incidence these characteristics deteriorate appreciably, cavitation occurring at about 40 knots at an incidence of 2 deg. for the thickness/chord ratio of 10 per cent.

For lifting surfaces one has to decide whether a high cavitation speed or a high loading at cavitation is required. A high cavitation speed can be attained by designing for a low lift coefficient and a small thickness/chord ratio, 65 knots being attainable with a good practical section designed for a lift coefficient of $0 \cdot 1$, and a thickness/chord ratio of 5 per cent, but the

6

loading would be only 8 lb/sq in. A high loading at cavitation can be attained by designing for a high lift coefficient and a small thickness/chord ratio, a loading of 15 lb/sq in. being attainable with a good practical section designed for a lift coefficient of 0·5 and a thickness/chord ratio of 5 per cent, but the cavitation speed would be only 40 knots.

For operation above cavitation speeds or over wide ranges of lift coefficients it is probable that sections other than those considered here would be better. Earlier cavitation might be acceptable provided that the characteristics above the cavitation speed were improved, but this would require further investigations.

APPENDIX I

Derivation of Symmetrical Sections

Assume that the section is defined by

$$x = \tfrac{1}{2}(1 - \cos \theta) \, , \qquad \qquad \left.\begin{matrix} \\ \\ \end{matrix}\right\} \qquad \qquad \qquad \qquad \qquad (1)$$
$$y = \sum_{1}^{\infty} A_n \sin n\theta \, .$$

By thin-aerofoil theory[1] the velocity distribution is given by

$$\frac{U}{U_0} = 1 + \frac{2}{\sin \theta} \sum_{1}^{\infty} n A_n \sin n\theta \, . \qquad \qquad \qquad \qquad \qquad (2)$$

We wish to derive a symmetrical section which will have a velocity distribution in which the velocity is constant over most of the chord, but falls off linearly at the leading and trailing edges. The velocity distribution can be written

$$\frac{U}{U_0} = 1 + (a - b) \frac{x}{x_1} + b, \qquad \text{for } 0 \leqslant x \leqslant x_1,\, 0 \leqslant \theta \leqslant \theta_1 \, , \qquad \left.\begin{matrix} \\ \\ \\ \\ \\ \end{matrix}\right\}$$

$$\frac{U}{U_0} = 1 + a, \qquad \text{for } x_1 \leqslant x \leqslant 1 - x_1,\, \theta_1 \leqslant \theta \leqslant \pi - \theta_1, \qquad \cdots \quad (3)$$

$$\frac{U}{U_0} = 1 + (a - b) \frac{1 - x}{x_1} + b, \quad \text{for } 1 - x_1 \leqslant x \leqslant 1,\, \pi - \theta_1 \leqslant \theta \leqslant \pi \, ,$$

Now from (2) the values of A_n in terms of the velocity distribution are given by

$$A_n = \frac{1}{\pi n} \int_0^{\pi} \left(\frac{U}{U_0} - 1 \right) \sin \theta \, \sin n\theta \, d\theta \, . \qquad \qquad \qquad \qquad (4)$$

Substituting for x from (1) into (3), and then for U/U_0 from (3) into (4) we obtain

$$A_1 = \tfrac{1}{2}a - \frac{a - b}{\pi x_1} \left(\tfrac{1}{24} \sin 3\theta_1 + \tfrac{3}{8} \sin \theta_1 - \tfrac{1}{2}\theta_1 \cos \theta_1 \right) ,$$

$$A_2 = A_4 = A_6 = \ldots = 0 \, ,$$

$$A_n \text{ (for } n = 3, 5, 7, \ldots) = - \frac{a - b}{\pi x_1} \left[\frac{n^2 + 2}{2n\,(n^2 - 1)(n^2 - 4)} \cos 2\theta_1 \sin n\theta_1 \right.$$

$$\left. - \frac{3}{2\,(n^2 - 1)(n^2 - 4)} \sin 2\theta_1 \cos n\theta_1 - \frac{1}{2n(n^2 - 1)} \sin n\theta_1 \right]$$

7

The three sections considered correspond to

$$\theta_1 = 25 \text{ deg } (x_1 = 0 \cdot 0432), \quad \theta_1 = 35 \text{ deg } (x_1 = 0 \cdot 0904), \quad \theta_1 = 45 \text{ deg } (x_1 = 0 \cdot 1464).$$

The condition for sharp leading and trailing edges is

$$\sum_1^\infty n A_n = 0,$$

which gives $\quad\quad \dfrac{a - b}{a \pi x_1} = 36 \cdot 5 \quad$ for $\theta_1 = 25$ deg

$$13 \cdot 65 \text{ for } \theta_1 = 35 \text{ deg}$$

$$6 \cdot 6 \quad \text{for } \theta_1 = 45 \text{ deg}$$

$$\hspace{8cm} \dots \quad \dots \quad \dots \quad \dots \quad (5)$$

With a as parameter the values of A_n can be determined using (5), and hence the section shape from (1). From (5) one can determine b, and hence, by substituting in (3) determine the precise velocity distribution in the regions of fall-off at the leading and trailing edges.

APPENDIX II

Derivation of Camber-Lines

The analysis is on the same lines as the thin-aerofoil theory given by Glauert, and quoted by Squire[1].

Let $U_0 k(x')dx'$ be the vorticity at the element of chord, dx', of the foil. $U_0 k(x')$ is equal to the difference in tangential velocity between the upper and lower surfaces. The induced velocity normal to the chord at the point x is given by

$$v(x) = \int_0^1 \frac{U_0 k(x')\, dx'}{2\pi(x' - x)} \cdot \hspace{4cm} \dots \quad \dots \quad \dots \quad \dots \quad \dots \quad \dots \quad \dots \quad (6)$$

The direction of the resultant velocity on the surface of the foil must be along the surface, and thus at each point of the foil we must have

$$\alpha + \frac{v}{U_0} = \frac{dy}{dx}, \hspace{4cm} \dots \quad \dots \quad \dots \quad \dots \quad \dots \quad \dots \quad \dots \quad (7)$$

where α is the angle of incidence, it being assumed that the induced velocity is a small fraction of the stream velocity everywhere.

We wish to derive a camber-line which, when set at a suitable angle of incidence, will have a velocity distribution in which the velocity is constant between two definite points, and falls linearly to the stream velocity at the leading and trailing edges. The velocity distribution on the upper surface can be written

$$\frac{U}{U_0} = 1 + \tfrac{1}{2}k_1 \frac{x'}{a}, \hspace{1cm} \text{for } 0 \leqslant x' \leqslant a,$$

$$\frac{U}{U_0} = 1 + \tfrac{1}{2}k_1, \hspace{1.7cm} \text{for } a \leqslant x' \leqslant b, \hspace{1cm} \dots \quad \dots \quad \dots \quad (8)$$

$$\frac{U}{U_0} = 1 + \tfrac{1}{2}k_1 \frac{1 - x'}{1 - b}, \hspace{0.6cm} \text{for } b \leqslant x' \leqslant 1.$$

8

There will be an equal-velocity decrement on the lower surface. The vorticity, or velocity difference, distribution is obtained by putting

$$
\left.
\begin{aligned}
k &= k_1 \frac{x'}{a}, && \text{for } 0 \leqslant x' \leqslant a , \\[4pt]
k &= k_1 , && \text{for } a \leqslant x' \leqslant b , \\[4pt]
k &= k_1 \frac{1 - x'}{1 - b}, && \text{for } b \leqslant x' \leqslant 1 .
\end{aligned}
\right\}
\qquad \dots \quad \dots \quad \dots \quad \dots \quad (9)
$$

By substituting for k from (9) in (6) to determine the induced normal velocity, we can determine the gradient at each point of the camber-line from (7). The equation of the camber-line can then be obtained by integration. The constant of integration and the value of α are chosen so that the leading and trailing edges of the camber-line lie on the x-axis. The value of α determined in this way is the ideal angle of incidence for which the velocity distribution will be as given by (8). The lift coefficient, C_L, at this incidence is related to k_1 by the relation

$$
C_L = \int_0^1 \frac{\varrho U_0{}^2 k(x') \, dx'}{\tfrac{1}{2}\varrho U_0{}^2} ,
$$

which, when integrated, gives

$$
k_1 = \frac{C_L}{1 + b - a} .
$$

With this value of k_1 the evaluation of the equation of the camber-line is

$$
\begin{aligned}
y = \frac{C_L}{2\pi(1 + b - a)} \Big\{ &\frac{(a - x)^2}{2a} \log |a - x| - \frac{x^2}{2a} \log x + \frac{(b - x)^2}{2(1 - b)} \log |b - x| \\
&- \frac{(1 - x)^2}{2(1 - b)} \log (1 - x) + g - hx \Big\} ,
\end{aligned}
$$

where

$$
g = - \tfrac{1}{2} a \log a - \frac{b^2}{2(1 - b)} \log b ,
$$

and

$$
h = g + \frac{(1 - a)^2}{2a} \log (1 - a) + \tfrac{1}{2}(1 - b) \log (1 - b) .
$$

The pitching-moment coefficient at zero lift for this camber-line is given by

$$
C_{m0} = \tfrac{1}{4} C_L - \int_0^1 \frac{\varrho U_0{}^2 k(x') x' \, dx'}{\tfrac{1}{2}\varrho U_0{}^2} ,
$$

which, when integrated, gives

$$
C_{m0} = - \frac{1 + 3a + b - 4a^2 + 4b^2}{12(1 + b - a)} C_L .
$$

REFERENCES

No.	Author	Title, etc.
1	H. B. Squire	Review of Calculations on Low Drag Wing Sections. A.R.C. 5865. April, 1942. (Unpublished.)
2	A. D. Young	A Survey of Compressibility Effects in Aeronautics. A.R.C. 5749. February, 1942. (Unpublished.)
3	T. Theodorsen	Theory of Wing Sections of Arbitrary Shape. N.A.C.A. T.R. No. 411. 1931.
4	H. B. Squire	Tables of Aerofoil Sections for High Speed Aircraft. R.A.E. Aero Memorandum No. 27. June, 1945.
5	E. N. Jacobs	Preliminary Report on Laminar-Flow Airfoils and New Methods adopted for Airfoil and Boundary-Layer Investigations. N.A.C.A. Advance Report No. W.R. L345. A.R.C. 5427. April, 1939.
6	B. Thwaites	On the Design of Aerofoil Sections for High Speed Aircraft. A.R.C. 9076. October, 1945. (Unpublished.)

TABLE 1

Ordinates of Preliminary Symmetrical Sections

θ (deg)	x	y		
		$\theta_1 = 25$ deg	$\theta_1 = 35$ deg	$\theta_1 = 45$ deg
0	0	0	0	0
10	0·0076	0·0013	0·0007	0·0004
20	0·0302	0·0094	0·0050	0·0031
25	0·0468	0·0155	—	—
30	0·0670	0·0209	0·0150	0·0096
35	0·0904	—	0·0208	—
40	0·1170	0·0290	0·0258	0·0198
45	0·1464	—	—	0·0252
50	0·1786	0·0358	0·0332	0·0296
60	0·25	0·0411	0·0390	0·0359
70	0·3290	0·0450	0·0430	0·0404
80	0·4132	0·0473	0·0455	0·0430
90	0·5	0·0481	0·0463	0·0439

TABLE 2

Ordinates of Symmetrical Sections (Thickness/Chord Ratio 10 per cent)

θ (deg)	x	y				
		Ellipse	25 deg Section	35 deg Section	45 deg Section	Circular Arc
0	0	0	0	0	0	0
10	0·0076	0·0087	0·0026	0·0019	0·0015	0·0015
20	0·0302	0·0171	0·0104	0·0075	0·0059	0·0059
25	0·0468	0·0211	0·0161	—	—	0·0089
30	0·0670	0·025	0·0217	0·0166	0·0131	0·0125
35	0·0904	0·0287	—	0·0225	—	0·0164
40	0·1170	0·0321	0·0302	0·0279	0·0229	0·0207
45	0·1464	0·0354	—	—	0·0287	0·025
50	0·1786	0·0383	0·0372	0·0358	0·0337	0·0293
60	0·25	0·0433	0·0427	0·0421	0·0409	0·0375
70	0·3290	0·0470	0·0467	0·0464	0·0460	0·0442
80	0·4132	0·0492	0·0492	0·0491	0·0490	0·0485
90	0·5	0·05	0·05	0·05	0·05	0·05
L.E. or T.E. radius		0·005	0	0	0	0
L.E. or T.E. angle		180 deg	38 deg	28 deg	22 deg	23 deg
$(U/U_0)_{max}$ at zero incidence		1·1	1·106	1·111	1·118	1·132

The 25 deg, 35 deg and 45 deg sections are straight from $\theta = 0$ to $\theta = 25$ deg, 35 deg and 45 deg respectively. All sections are symmetrical about horizontal and vertical axes through the centre.

TABLE 3

Ordinates of Camber-lines (Design $C_L = 1 \cdot 0$)

$0 \cdot 05$ *Series* (i.e., $a = 0 \cdot 05$)

x	Camber-line						
	$(0 \cdot 05\text{–}0 \cdot 5)$	$(0 \cdot 05\text{–}0 \cdot 6)$	$(0 \cdot 05\text{–}0 \cdot 7)$	$(0 \cdot 05\text{–}0 \cdot 8)$	$(0 \cdot 05\text{–}0 \cdot 85)$	$(0 \cdot 05\text{–}0 \cdot 9)$	$(0 \cdot 05\text{–}0 \cdot 95)$
	y						
0	0	0	0	0	0	0	0
0·0125	0·00606	0·00571	0·00536	0·00503	0·00486	0·00469	0·00452
0·025	0·01251	0·01178	0·01107	0·01039	0·01004	0·00969	0·00933
0·05	0·02492	0·02347	0·02206	0·02070	0·02002	0·01933	0·01861
0·075	0·03427	0·03229	0·03037	0·02848	0·02754	0·02657	0·02556
0·1	0·04183	0·03946	0·03714	0·03482	0·03365	0·03246	0·03120
0·15	0·05398	0·05105	0·04810	0·04504	0·04355	0·04195	0·04024
0·2	0·06335	0·06009	0·05669	0·05316	0·05131	0·04938	0·04729
0·25	0·07058	0·06718	0·06350	0·05957	0·05748	0·05527	0·05285
0·3	0·07598	0·07263	0·06882	0·06460	0·06232	0·05988	0·05717
0·35	0·07966	0·07659	0·07280	0·06842	0·06600	0·06337	0·06042
0·4	0·08169	0·07914	0·07553	0·07111	0·06860	0·06583	0·06268
0·45	0·08200	0·08029	0·07706	0·07274	0·07019	0·06733	0·06402
0·5	0·08027	0·08000	0·07738	0·07331	0·07079	0·06788	0·06446
0·55	0·07589	0·07813	0·07646	0·07282	0·07039	0·06756	0·06402
0·6	0·06971	0·07428	0·07418	0·07122	0·06897	0·06618	0·06268
0·65	0·06228	0·06768	0·07036	0·06844	0·06647	0·06385	0·06042
0·7	0·05394	0·05935	0·06448	0·06432	0·06278	0·06045	0·05717
0·75	0·04497	0·04993	0·05571	0·05859	0·05774	0·05585	0·05285
0·8	0·03562	0·03982	0·04503	0·05059	0·05101	0·04984	0·04729
0·85	0·02613	0·02937	0·03356	0·03902	0·04179	0·04203	0·04024
0·9	0·01680	0·01896	0·02181	0·02582	0·02850	0·03139	0·03120
0·95	0·00791	0·00895	0·01034	0·01234	0·01379	0·01580	0·01861
1·0	0	0	0	0	0	0	0
Ideal angle of incidence (deg)	2·44	2·01	1·53	1·00	0·70	0·38	0
$- C_{m0}$	0·152	0·171	0·192	0·214	0·226	0·238	0·25
$(U/U_0)_{max}$ at ideal angle of incidence	1·345	1·323	1·303	1·286	1·278	1·270	1·263

TABLE 4

Ordinates of Camber-lines (Design $C_L = 1 \cdot 0$)

0·1 *Series* (i.e., $a = 0 \cdot 1$)

x	Camber-line					
	(0·1—0·5)	(0·1—0·6)	(0·1—0·7)	(0·1—0·8)	(0·1—0·85)	(0·1—0·9)
	y					
0	0	0	0	0	0	0
0·0125	0·00500	0·00471	0·00441	0·00412	0·00398	0·00383
0·025	0·01034	0·00973	0·00912	0·00854	0·00823	0·00792
0·05	0·02145	0·02016	0·01892	0·01770	0·01706	0·01646
0·075	0·03242	0·03051	0·02865	0·02681	0·02588	0·02494
0·1	0·04245	0·03997	0·03754	0·03513	0·03392	0·03268
0·15	0·05683	0·05362	0·05041	0·04718	0·04554	0·04383
0·2	0·06729	0·06366	0·05994	0·05610	0·05412	0·05206
0·25	0·07518	0·07136	0·06730	0·06303	0·06078	0·05842
0·3	0·08096	0·07718	0·07296	0·06838	0·06593	0·06332
0·35	0·08487	0·08135	0·07714	0·07238	0·06978	0·06697
0·4	0·08698	0·08399	0·07997	0·07516	0·07245	0·06951
0·45	0·08725	0·08514	0·08149	0·07679	0·07405	0·07100
0·5	0·08536	0·08474	0·08174	0·07729	0·07458	0·07149
0·55	0·08072	0·08268	0·08067	0·07668	0·07407	0·07100
0·6	0·07412	0·07855	0·07818	0·07490	0·07248	0·06951
0·65	0·06624	0·07156	0·07407	0·07188	0·06976	0·06697
0·7	0·05739	0·06276	0·06784	0·06747	0·06580	0·06332
0·75	0·04788	0·05281	0·05850	0·06139	0·06043	0·05842
0·8	0·03796	0·04214	0·04737	0·05296	0·05333	0·05206
0·85	0·02789	0·03111	0·03533	0·04075	0·04364	0·04383
0·9	0·01795	0·02010	0·02297	0·02703	0·02976	0·03268
0·95	0·00847	0·00951	0·01091	0·01294	0·01441	0·01646
1·0	0	0	0	0	0	0
Ideal angle of incidence (deg)	2·03	1·61	1·15	0·62	0·33	0
$- C_{m0}$	0·164	0·183	0·204	0·226	0·238	0·25
$(U/U_0)_{max}$ at ideal angle of incidence	1·357	1·333	1·312	1·294	1·286	1·278

TABLE 5

Ordinates of Camber-lines $(Design\ C_L = 1\cdot0)$

$0\cdot15$ *Series* (i.e., $a = 0\cdot15$)

x	Camber-line				
	$(0\cdot15\text{--}0\cdot5)$	$(0\cdot15\text{--}0\cdot6)$	$(0\cdot15\text{--}0\cdot7)$	$(0\cdot15\text{--}0\cdot8)$	$(0\cdot15\text{--}0\cdot85)$
			y		
0	0	0	0	0	0
0·0125	0·00442	0·00415	0·00388	0·00362	0·00348
0·025	0·00910	0·00855	0·00800	0·00747	0·00719
0·05	0·01896	0·01781	0·01670	0·01556	0·01500
0·075	0·02905	0·02730	0·02558	0·02387	0·02301
0·1	0·03902	0·03669	0·03439	0·03210	0·03095
0·15	0·05706	0·05372	0·05041	0·04708	0·04539
0·2	0·06949	0·06559	0·06162	0·05757	0·05549
0·25	0·07841	0·07424	0·06987	0·06531	0·06293
0·3	0·08484	0·08066	0·07608	0·07117	0·06856
0·35	0·08915	0·08521	0·08062	0·07550	0·07273
0·4	0·09148	0·08808	0·08366	0·07848	0·07560
0·45	0·09182	0·08932	0·08529	0·08021	0·07729
0·5	0·08988	0·08892	0·08556	0·08074	0·07785
0·55	0·08499	0·08676	0·08442	0·08008	0·07729
0·6	0·07812	0·08242	0·08180	0·07820	0·07560
0·65	0·06985	0·07510	0·07747	0·07501	0·07273
0·7	0·06056	0·06589	0·07093	0·07037	0·06856
0·75	0·05055	0·05547	0·06117	0·06399	0·06293
0·8	0·04011	0·04429	0·04955	0·05518	0·05549
0·85	0·02950	0·03273	0·03697	0·04256	0·04539
0·9	0·01901	0·02116	0·02406	0·02818	0·03095
0·95	0·00899	0·01003	0·01144	0·01350	0·01500
1·0	0	0	0	0	0
Ideal angle of incidence (deg)	1·68	1·27	0·81	0·29	0
$- C_{m0}$	0·177	0·195	0·216	0·238	0·25
$(U/U_0)_{max}$ at ideal angle of incidence	1·370	1·345	1·323	1·303	1·294

14

TYPICAL SECTION WITH VELOCITY DISTRIBUTION

VELOCITY ON UPPER SURFACE

VELOCITY ON LOWER SURFACE

CORRESPONDING SYMMETRICAL SECTION WITH VELOCITY DISTRIBUTION

VELOCITY ON EITHER SURFACE

CAMBER LINE WITH VELOCITY DISTRIBUTION

VELOCITY ON UPPER SURFACE

VELOCITY ON LOWER SURFACE

$$y_u = y_c + y_t \qquad u_u = u_t + u_c$$
$$y_l = y_c - y_t \qquad u_l = u_t - u_c$$
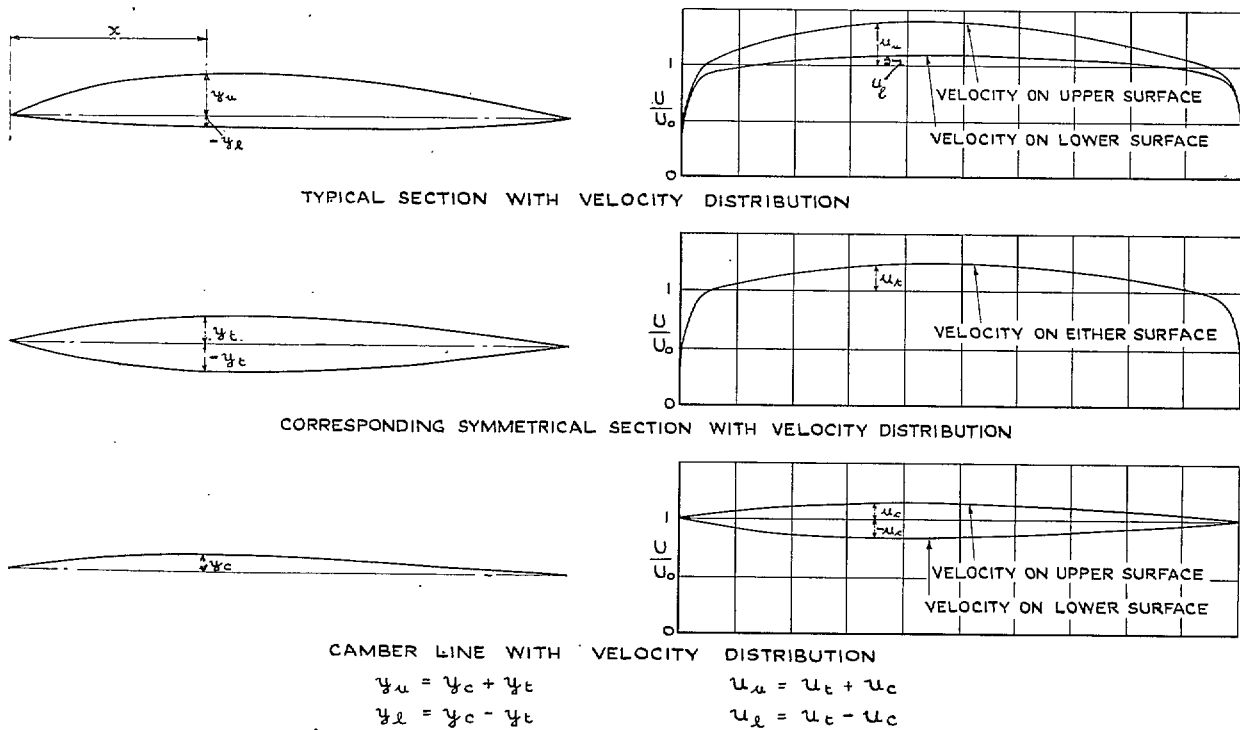
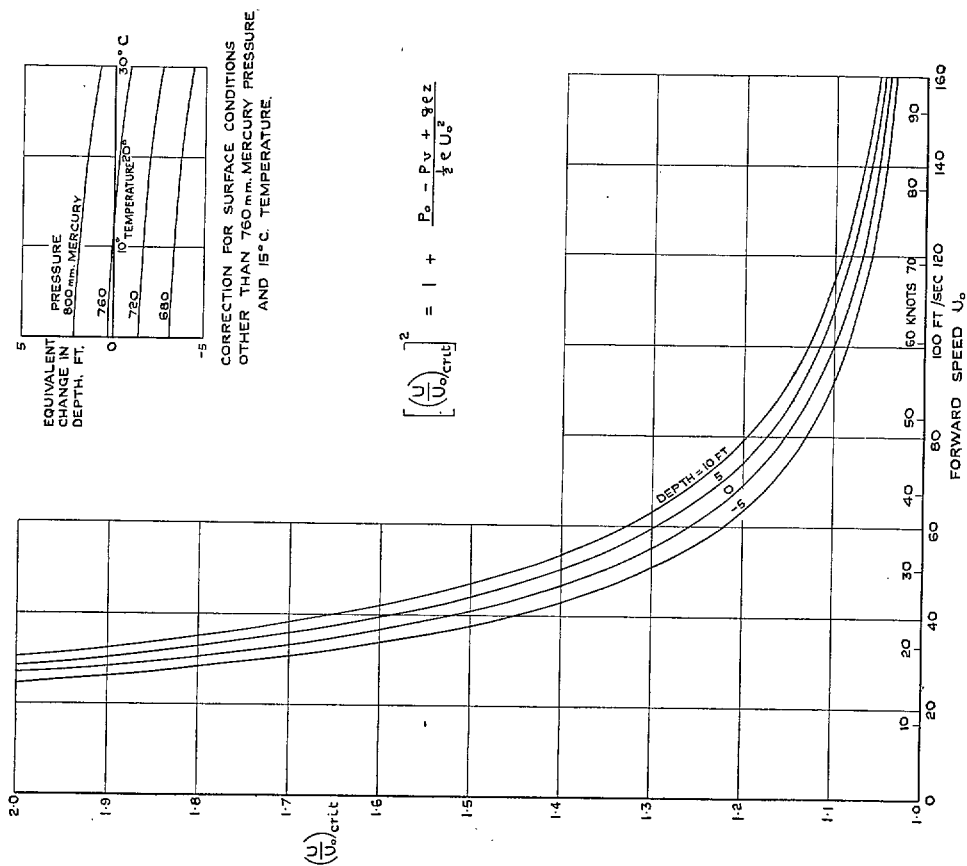FIG. 1. Illustration of the breakdown of a typical section into a symmetrical section superimposed on a camber-line.

$$\left[\frac{U}{U_0}\right]_{crit}^2 = 1 + \frac{P_0 - P_v + gρz}{\frac{1}{2}ρU_0^2}$$

FIG. 2. Critical local velocity ratio in terms of forward speed and depth.
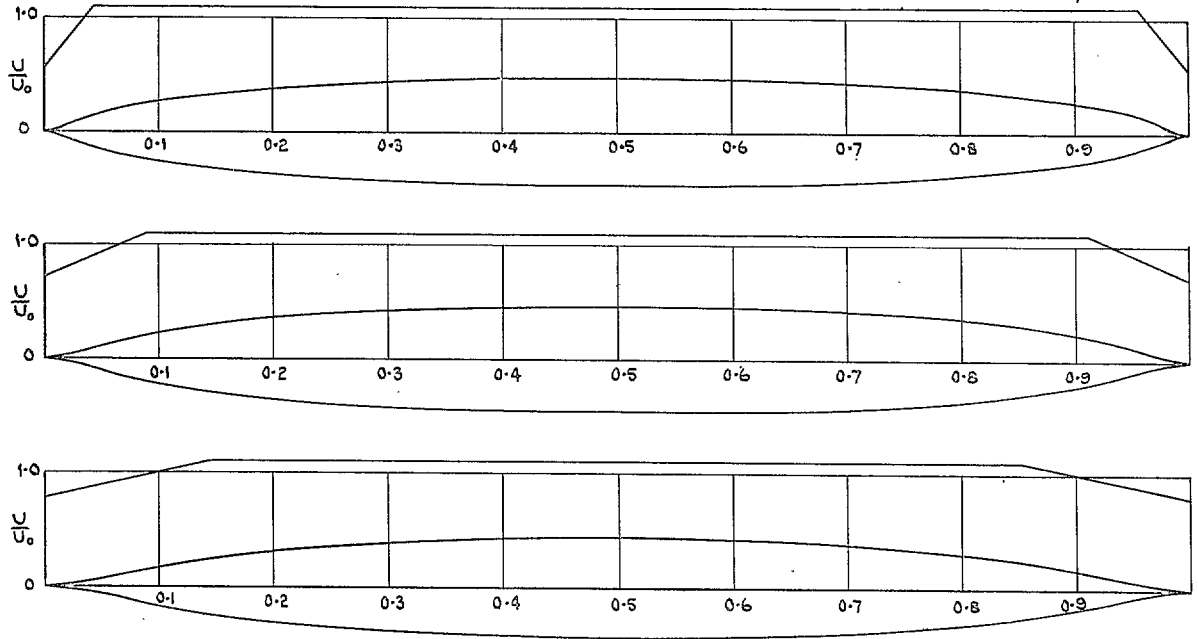
FIG. 3.   Preliminary symmetrical sections having cuspidal leading and trailing edges, with the prescribed velocity distributions.
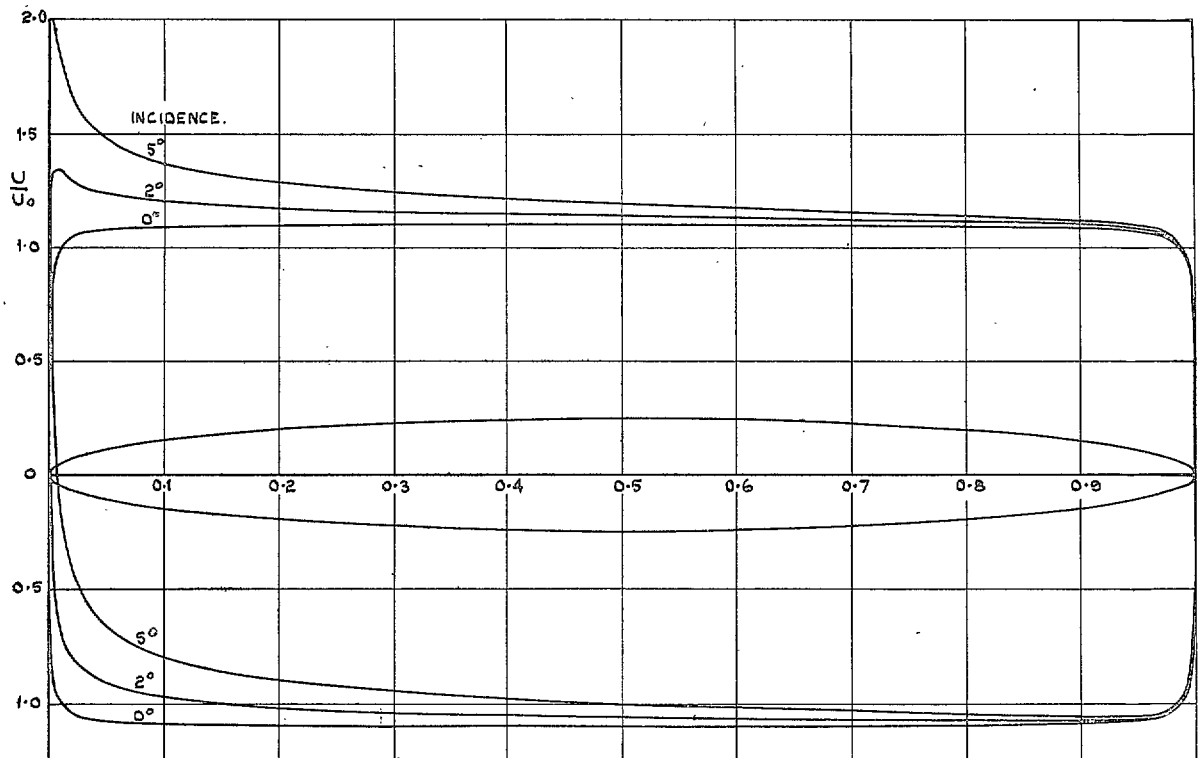
FIG. 4.   Velocity distribution on an elliptic section.

16
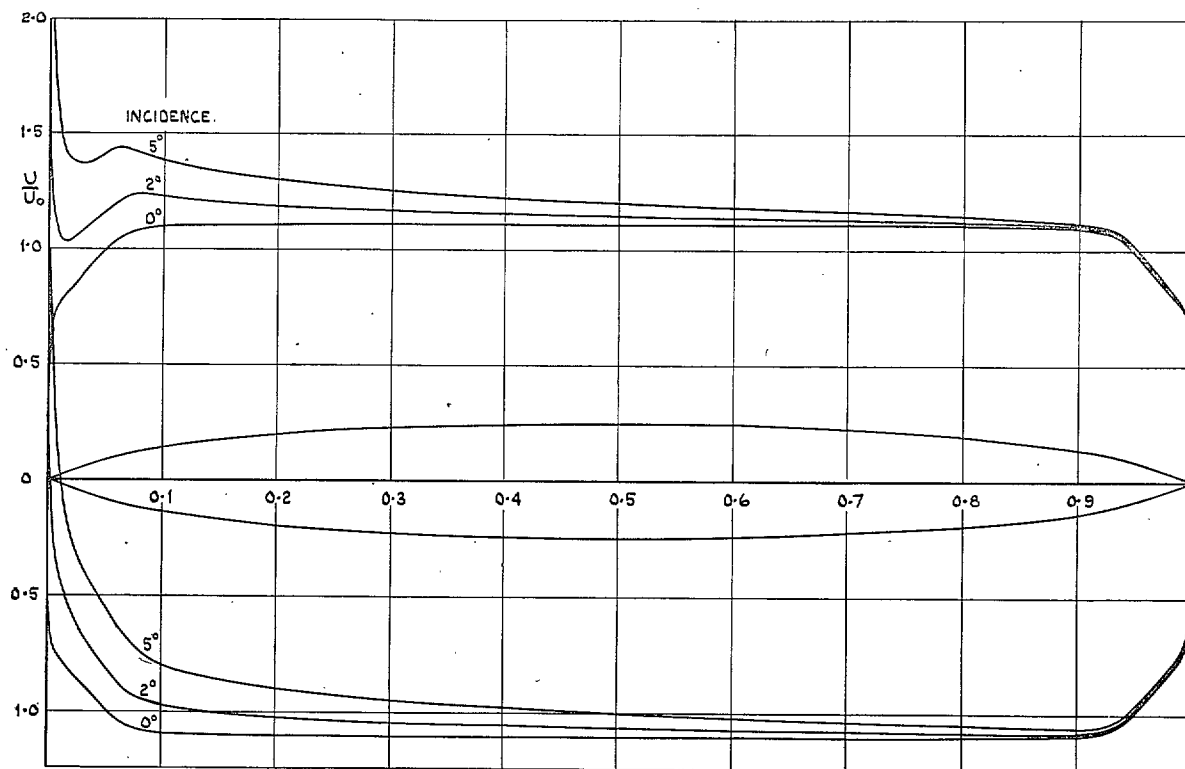
FIG. 5. Velocity Distribution on the 25 deg section.
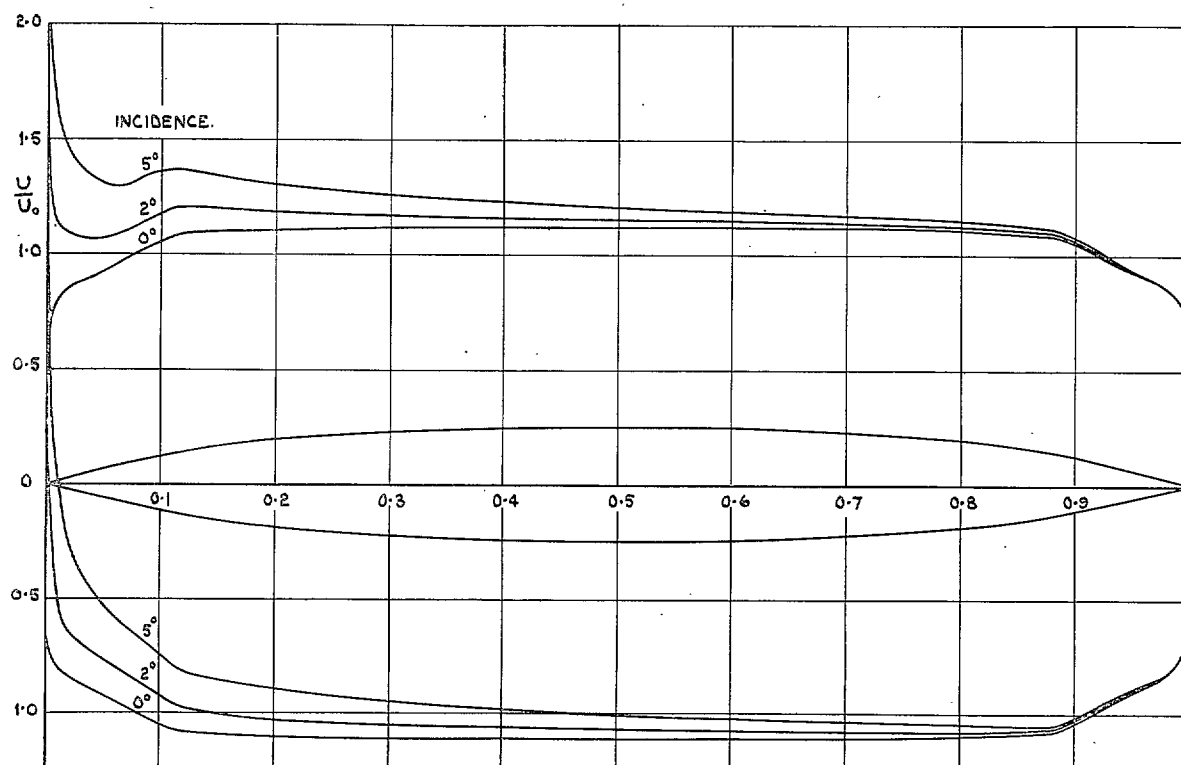
FIG. 6. Velocity distribution on the 35 deg section.

17
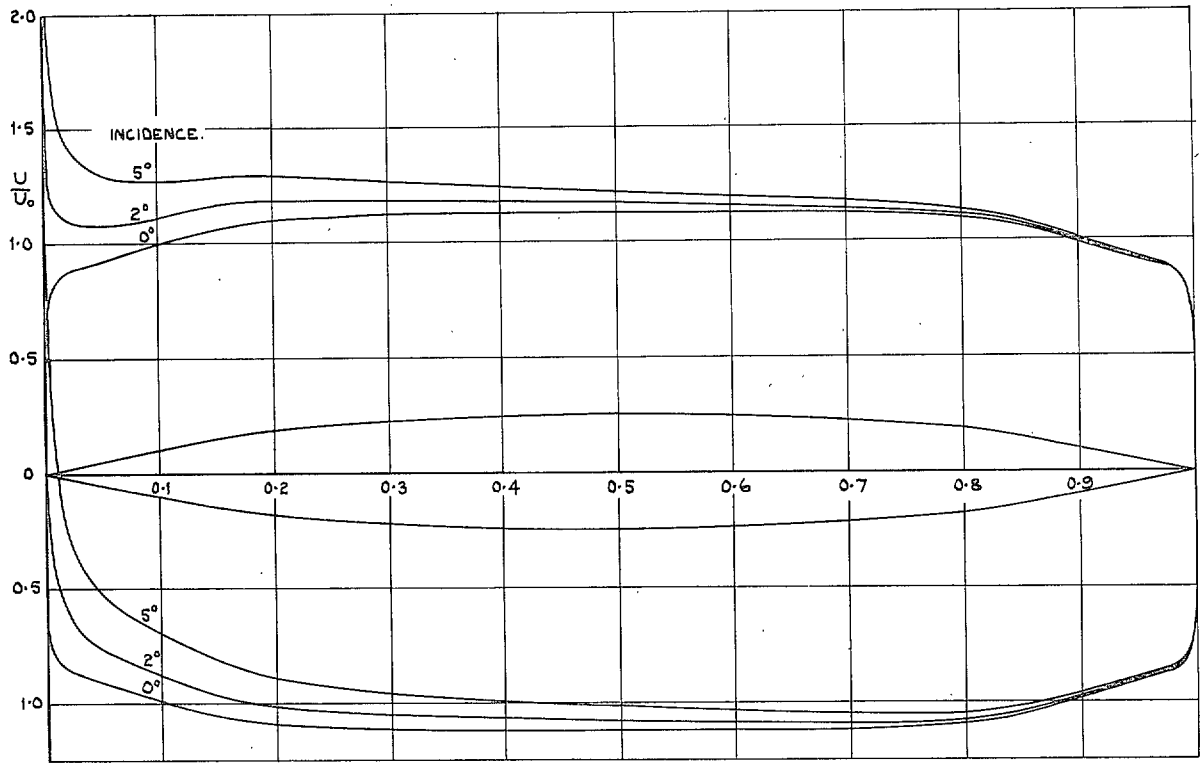
Fig. 7. Velocity distribution on the 45 deg section.
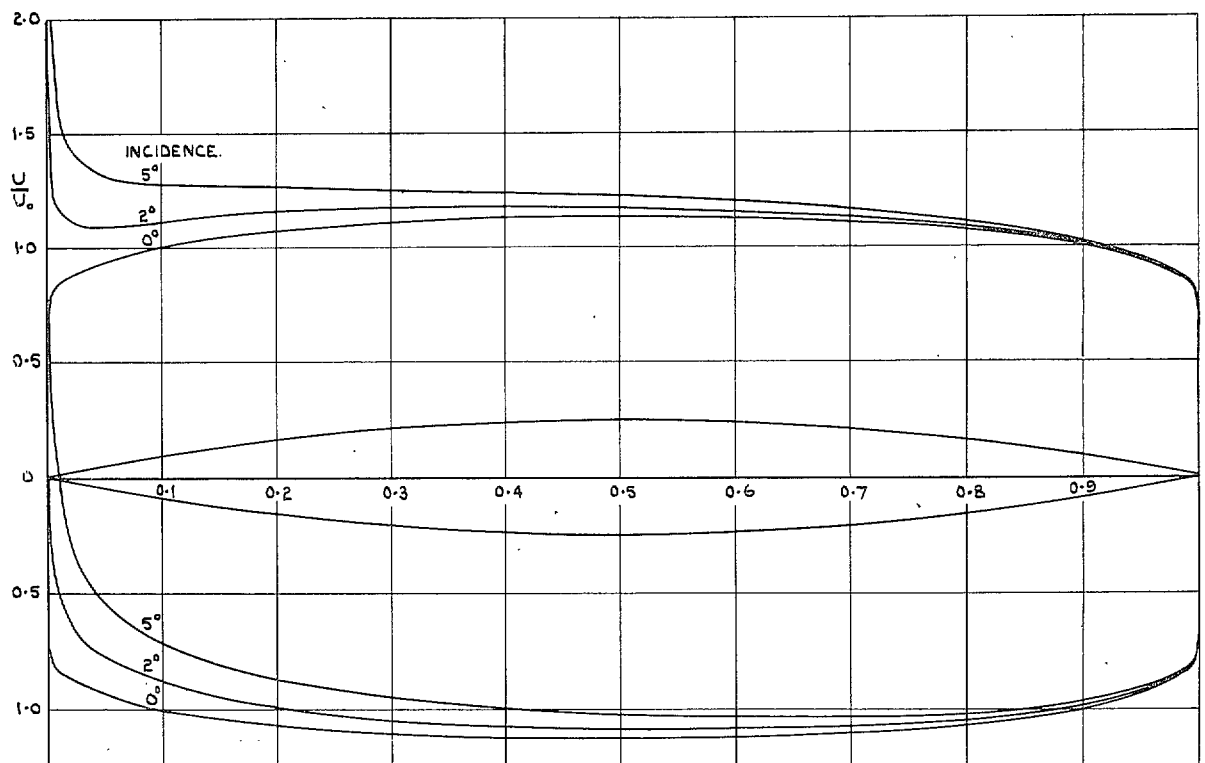
Fig. 8. Velocity distribution on a circular-arc section.

18
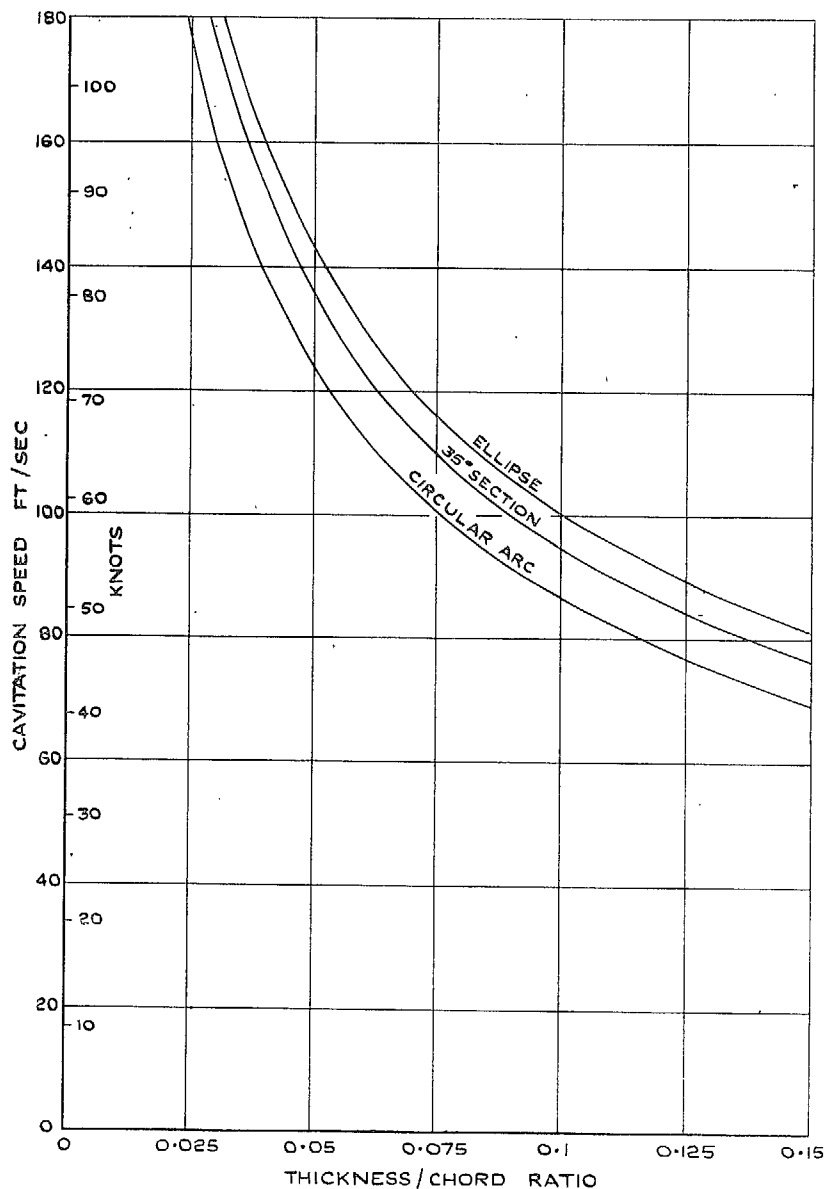
FIG. 9.   The cavitation speed at zero incidence for three symmetrical
sections in terms of the thickness/chord ratio.
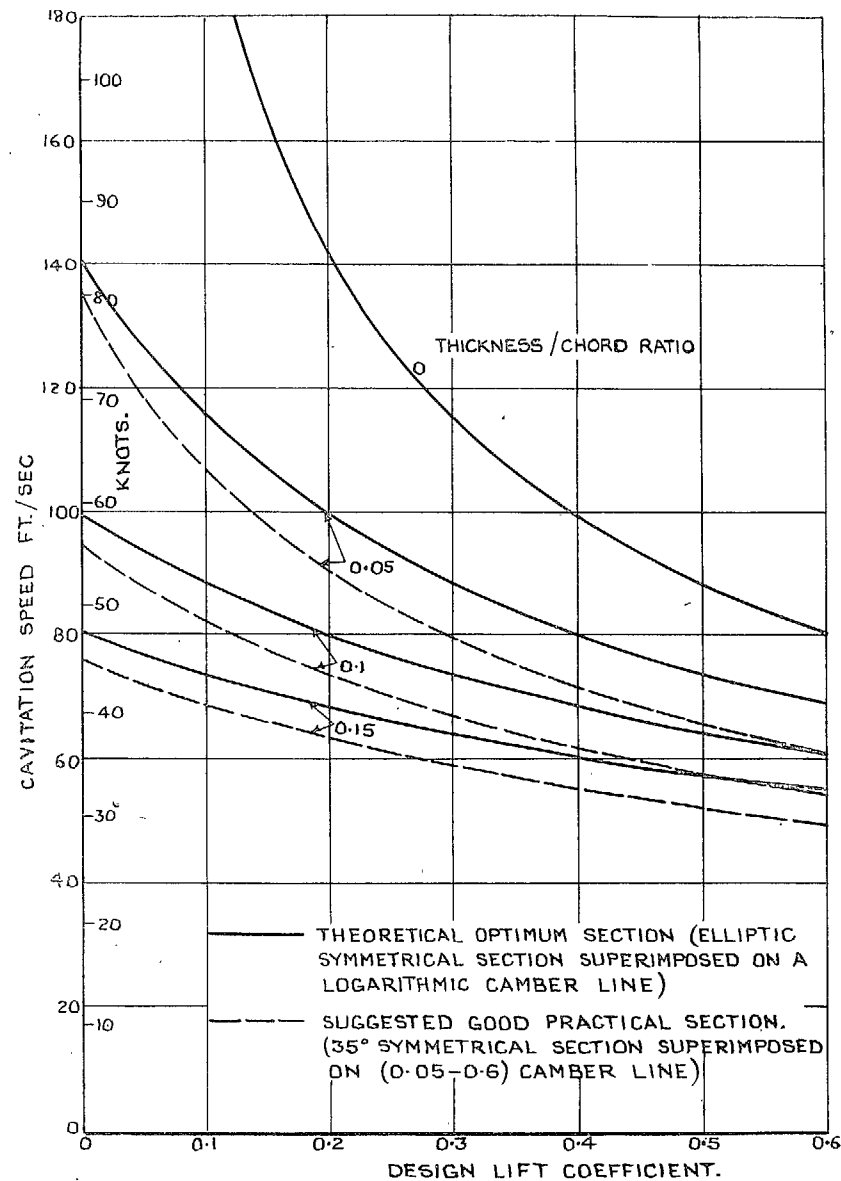
FIG. 10.   The cavitation speed at the ideal angle of incidence for two
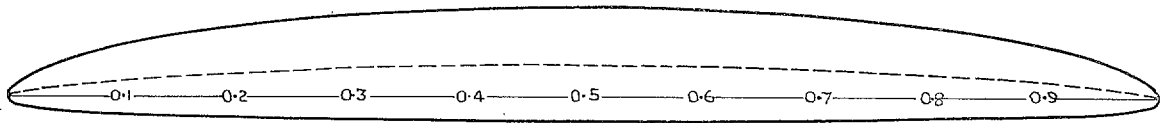series of section in terms of the thickness/chord ratio and design lift
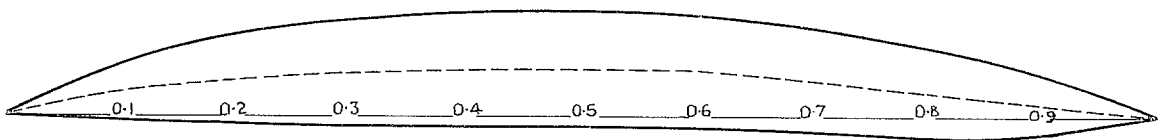coefficient.
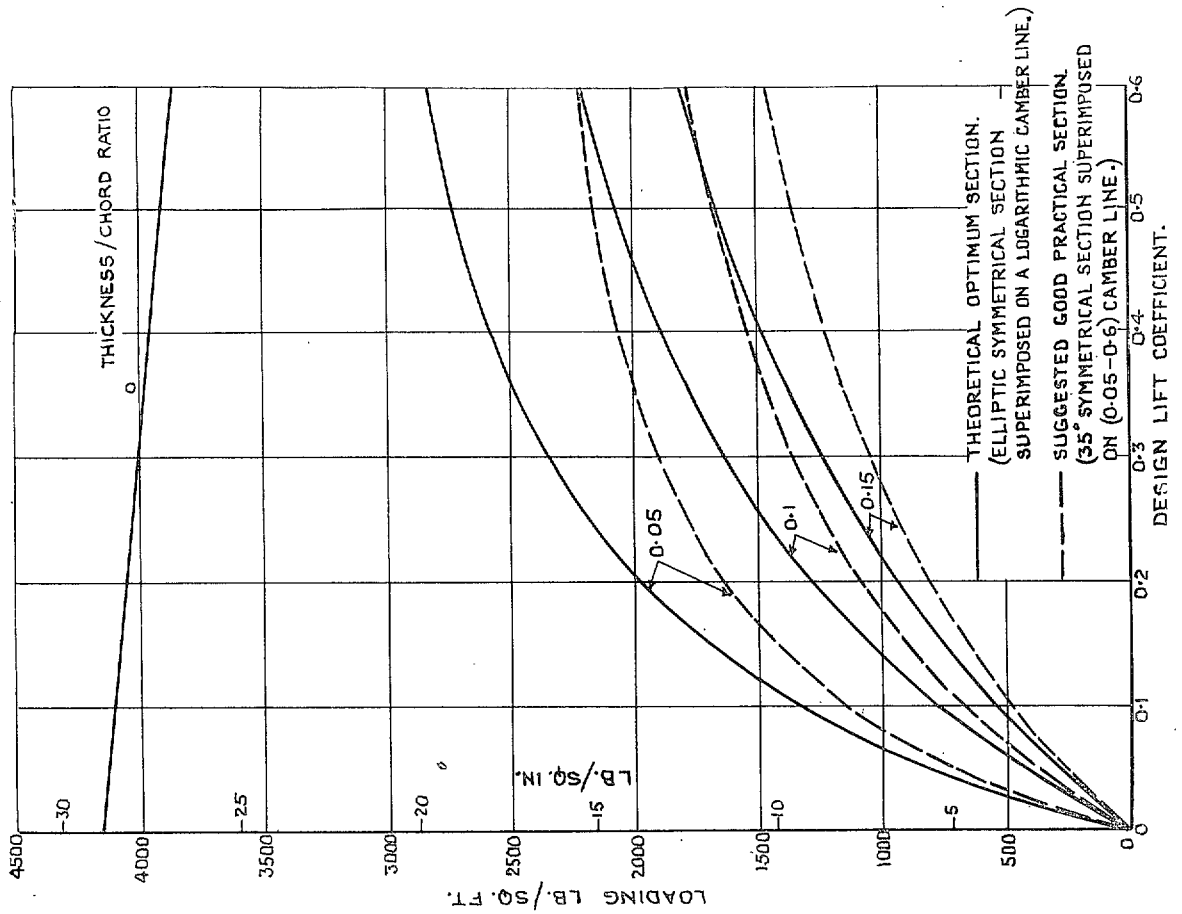
FIG. 11. The cavitation loading at the ideal angle of incidence for two series of section in terms of the thickness/chord ratio and design lift coefficient.

ELLIPTIC SYMMETRICAL SECTION SUPERIMPOSED ON A LOGARITHMIC CAMBER LINE.
(IDEAL ANGLE OF INCIDENCE = 0°)

35° SYMMETRICAL SECTION SUPERIMPOSED ON (0·05−0·6) CAMBER LINE
(IDEAL ANGLE OF INCIDENCE = 2°).

FIG. 12.   Comparison of two sections having a thickness/chord ratio of 10 per cent and designed for a lift coefficient of 0·5.

20

Publications of the
Aeronautical Research Council

ANNUAL TECHNICAL REPORTS OF THE AERONAUTICAL RESEARCH COUNCIL (BOUND VOLUMES)

1936 Vol. I. Aerodynamics General, Performance, Airscrews, Flutter and Spinning. 40s. (40s. 9d.)
    Vol. II. Stability and Control, Structures, Seaplanes, Engines, etc. 50s. (50s. 10d.)

1937 Vol. I. Aerodynamics General, Performance, Airscrews, Flutter and Spinning. 40s. (40s. 10d.)
    Vol. II. Stability and Control, Structures, Seaplanes, Engines, etc. 60s. (61s.)

1938 Vol. I. Aerodynamics General, Performance, Airscrews. 50s. (51s.)
    Vol. II. Stability and Control, Flutter, Structures, Seaplanes, Wind Tunnels, Materials. 30s. (30s. 9d.)

1939 Vol. I. Aerodynamics General, Performance, Airscrews, Engines. 50s. (50s. 11d.)
    Vol. II. Stability and Control, Flutter and Vibration, Instruments, Structures, Seaplanes, etc. 63s. (64s. 2d.)

1940 Aero and Hydrodynamics, Aerofoils, Airscrews, Engines, Flutter, Icing, Stability and Control, Structures, and a miscellaneous section. 50s. (51s.)

1941 Aero and Hydrodynamics, Aerofoils, Airscrews, Engines, Flutter, Stability and Control, Structures. 63s. (64s. 2d.)

1942 Vol. I. Aero and Hydrodynamics, Aerofoils, Airscrews, Engines. 75s. (76s. 3d.)
    Vol. II. Noise, Parachutes, Stability and Control, Structures, Vibration, Wind Tunnels. 47s. 6d. (48s. 5d.)

1943 Vol. I. (In the press.)
    Vol. II. (In the press.)

ANNUAL REPORTS OF THE AERONAUTICAL RESEARCH COUNCIL—

1933–34	1s. 6d. (1s. 8d.)	1937	2s. (2s. 2d.)
1934–35	1s. 6d. (1s. 8d.)	1938	1s. 6d. (1s. 8d.)
April 1, 1935 to Dec. 31, 1936.	4s. (4s. 4d.)	1939–48	3s. (3s. 2d.)

INDEX TO ALL REPORTS AND MEMORANDA PUBLISHED IN THE ANNUAL TECHNICAL REPORTS, AND SEPARATELY—

April, 1950 - - - - R. & M. No. 2600. 2s. 6d. (2s. 7½d.)

AUTHOR INDEX TO ALL REPORTS AND MEMORANDA OF THE AERONAUTICAL RESEARCH COUNCIL—

1909–1949. R. & M. No. 2570. 15s. (15s. 3d.)

INDEXES TO THE TECHNICAL REPORTS OF THE AERONAUTICAL RESEARCH COUNCIL—

December 1, 1936 — June 30, 1939.	R. & M. No. 1850.	1s. 3d. (1s. 4½d.)
July 1, 1939 — June 30, 1945.	R. & M. No. 1950.	1s. (1s. 1½d.)
July 1, 1945 — June 30, 1946.	R. & M. No. 2050.	1s. (1s. 1½d.)
July 1, 1946 — December 31, 1946.	R. & M. No. 2150.	1s. 3d. (1s. 4½d.)
January 1, 1947 — June 30, 1947.	R. & M. No. 2250.	1s. 3d. (1s. 4½d.)
July, 1951.	R. & M. No. 2350.	1s. 9d. (1s. 10½d.)

Prices in brackets include postage.

Obtainable from

HER MAJESTY'S STATIONERY OFFICE